Proceedings of the 4th International Conference on Software Engineering and Machine Learning
DOI: 10.54254/2755-2721/2026.34321

Research on Low-Carbon Intelligent Machining Path Planning Method for Lightweight Composite Materials of Aerospace Components Toward Green Manufacturing

Siyi Wang

City University of Hong Kong, Hong Kong, China
rara481846778@gmail.com

Abstract. The work offers a methodology for low-carbon intelligent path planning in machining operations of carbon fiber reinforced polymers used in aerospace parts. In this case, the object of research is a lightweight bracket made from a carbon composite material with an irregular profile, two different slots, and areas of variable thickness. A set of 30 samples of such brackets was developed using Siemens NX 2306 software. Machining data have been collected on a VMC 850 machine equipped with Yokogawa WT5000 energy meter with a period of data sampling of 0.1 seconds. Genetic algorithm path optimization was carried out in MATLAB R2024a software, whereas data processing and computation of carbon footprint values was done with Python 3.11. The comparison of optimized paths was done against reference trajectories provided by Siemens NX under equal conditions of tools, spindles, feeds, depth of cuts, and inspections. Optimization showed a path shorter by 286.4 ± 42.7 mm, travel distance by 214.8 ± 36.5 mm, machining duration by 18.6 ± 3.9 seconds, energy consumed by 0.184 ± 0.037 kWh, and carbon emissions by 0.105 ± 0.021 kg CO2, with surface roughness being unchanged at 1.42 ± 0.16 μm.

Keywords: Low-carbon machining, path planning, lightweight composite materials, aerospace components, green manufacturing

1. Introduction

The lightweight composite materials are commonly used in the aerospace structure as they decrease the weight of a component but do not compromise with the high specific strength, fatigue, and corrosion resistance. Carbon fiber reinforced polymer parts are particularly prevalent in brackets, panels, ribs, fairings, and secondary load bearing structures where geometrical precision and surface integrity is needed following post-forming machining [1, 2]. Although many composite parts are close to their final shape after molding, trimming, slot milling, contour correction, and edge finishing are still necessary for assembly accuracy and functional reliability.

Machining aerospace composite components creates a direct link between geometric path planning, energy consumption, and surface quality. Tool paths determine cutting distance, non-cutting travel, corner transitions, feed-axis movement, and spindle working time. These factors influence the electrical energy consumed by the machining center and the carbon emissions

© 2026 The Authors. This is an open access article distributed under the terms of the Creative Commons Attribution License 4.0 (https://creativecommons.org/licenses/by/4.0/).

DOI: 10.54254/2755-2721/2026.34321

associated with electricity use [3, 4]. Conventional CAM-generated tool paths primarily emphasize geometric completion, collision avoidance, and processing feasibility. Low-carbon objectives such as power fluctuation, idle motion, and carbon-equivalent output are usually calculated after machining rather than embedded into path generation.

Recent studies on sustainable machining, CNC toolpath optimization, and carbon-emission modeling show that machining time, energy consumption, and surface quality must be evaluated together rather than separately [5, 6]. For CFRP components, this requirement is stricter because abrupt path transitions and poor cutting continuity may increase energy use while also creating burrs, fiber pull-out, or edge defects. Therefore, path planning for aerospace composite components should integrate geometric coverage, motion continuity, energy modeling, carbon calculation, and quality constraints in one workflow.

This study proposes a low-carbon intelligent machining path planning framework for CFRP aerospace brackets. It constructs a fixed computational and experimental route covering geometric modeling, machining-region extraction, path representation, carbon-related objective modeling, genetic-algorithm optimization, machine-side power measurement, and comparative evaluation. The objective is to reduce energy consumption and carbon emission while maintaining surface roughness and edge integrity.

2. Literature review

2.1. Machining characteristics of aerospace composite components

Aerospace composite components usually contain curved contours, thin walls, laminated structures, variable-thickness regions, and local slots. These geometric features increase the difficulty of machining because tool engagement changes continuously during trimming and milling. CFRP materials also have anisotropic and heterogeneous structures, so machining defects such as burrs, delamination, fiber pull-out, matrix cracking, and surface roughness variation may appear under unsuitable tool paths or cutting conditions [2, 3]. Surface integrity is a core quality requirement in aerospace composite machining. Edge trimming and slot machining must control both geometric accuracy and damage formation. Path discontinuity, frequent direction changes, and abrupt corner transitions can increase cutting instability and local defect length.

2.2. Intelligent path planning in composite material processing

Intelligent path planning uses geometric modeling, node sequencing, optimization algorithms, and machine constraints to generate executable machining trajectories. For composite processing, the path must cover contours and slot regions, avoid collision, maintain continuous motion, and reduce unnecessary linking travel [5]. Path variables include the starting point, cutting direction, machining order, entry position, linking path, and corner transition strategy. Genetic algorithms and multi-objective optimization methods are suitable for this type of problem because machining path planning contains both discrete sequencing decisions and continuous geometric constraints. In low-carbon machining, optimization must also include energy consumption, carbon emission, and machining time rather than only length or feasibility [6, 7].

DOI: 10.54254/2755-2721/2026.34321

2.3. Low-carbon targets in green manufacturing

Low-carbon manufacturing requires measurable carbon accounting during machining. Electricity-driven CNC machining produces carbon emissions indirectly through electrical energy consumption, which is affected by spindle operation, feed-axis motion, rapid traverse, standby duration, and total processing time [6-8]. Therefore, a carbon-aware path model must separate cutting energy, linking energy, idle energy, and rapid-traverse energy. Green manufacturing research increasingly treats carbon emissions, efficiency, and quality as coupled objectives. Reducing path length may lower time, but it may also increase sharp turns or surface defects if transition constraints are ignored. A complete low-carbon path planning framework should therefore combine path geometry, energy calculation, carbon conversion, and final surface-quality evaluation [9, 10].

3. Experimental methodology

3.1. Workpiece modeling and dataset construction

The sample is an aerospace bracket made of carbon-fiber-reinforced polymer that has one curved outer contour, two internal slot features, and one variable-thickness section. Geometric model is designed using the software Siemens NX 2306 and exported into STEP format. It has 30 bracket models that belong to the same part family. Geometric variables are outer-contour curvature radius, slot length, slot spacing, complexity of the boundary and local thickness variation. Curvature radius is limited to 35-85mm, slot length is constrained to 28-46mm and maximum local thickness is between 4.2-7.8mm.

All parts are machined on the same machine setup, using the same fixture position, type of tools, spindle speed, feed rate and depth of the cut. The machining station is a three-axis VMC 850 machining station, which has a 6 mm polycrystalline diamond end mill. The spindle speed remains constant at 9000 rpm, feed rate at 1200 mm/min, axial depth of cut at 1.0 mm and radial depth of cut at 2.0 mm. Siemens NX produces the reference tool paths of each model that consist of contour trimming and slot milling sections. The amount of power used is measured by a Yokogawa WT5000 power analyzer every 0.1 second. CNC motion logs are exported after each run and include tool-center coordinates, feed state, rapid traverse state, spindle operation time, and segment identifiers. Surface roughness is measured after machining with a Mitutoyo SJ-210 roughness tester, and edge quality photographs are collected using a Keyence VHX-7000 digital microscope. All records are linked by model ID, trial ID, tool-path type, and timestamp.

3.2. Path representation and carbon-related objective modeling

The machining path is represented as an ordered sequence of tool-center points. Each complete path is divided into four segment types: cutting path, linking path, entry path, and exit path. Cutting paths remove material along contours or slots (see Figure 1). Linking paths connect local machining regions without cutting. Entry and exit paths describe cutter engagement and disengagement. In MATLAB R2024a, each tool path is stored as a structured matrix containing point coordinates, segment labels, feed status, transition angle, local curvature, and machining-region ID.

DOI: 10.54254/2755-2721/2026.34321

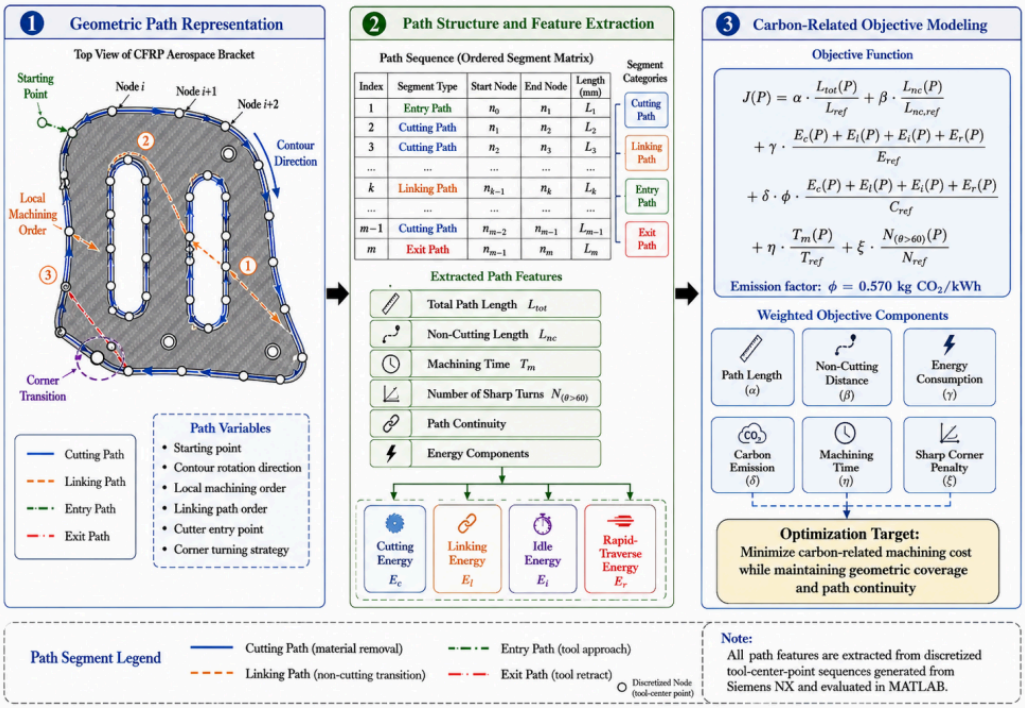

Figure 1. Path representation and carbon-related objective modeling

Local machining regions are extracted from contour and slot boundaries. Sharp corners are identified when adjacent segment angle change exceeds 45°. Non-cutting length is calculated from linking and rapid-traverse segments. The carbon-related path objective is formulated as shown in Equation (1):

$$J(P)=\alpha\frac{L_{tot}(P)}{L_{ref}}+\beta\frac{L_{nc}(P)}{L_{nc,ref}}+\gamma\frac{E_c(P)+E_l(P)+E_i(P)+E_r(P)}{E_{ref}}$$

$$+\delta\frac{\phi[E_c(P)+E_l(P)+E_i(P)+E_r(P)]}{C_{ref}}+\eta\frac{T_m(P)}{T_{ref}}+\xi\frac{N_{\theta>60}(P)}{N_{ref}} \quad (1)$$

where P denotes one candidate path, L_{tot} is total path length, L_{nc} is non-cutting length, E_c, E_l, E_i, and E_r denote cutting, linking, idle, and rapid-traverse energy, ϕ =0.570 kg CO_2/kWh is the fixed emission factor, T_m is machining time, and $N_{\theta>60}$ is the number of corner transitions exceeding 60 degrees. The weights are set as α =0.15, β =0.20, γ =0.25, δ =0.25, η =0.10, and ξ =0.05.

3.3. Planning algorithm and constraint setting

The tool-path optimization process follows a genetic algorithm fixed on a population size of 80, 120 generations, 0.85 crossover, 0.08 mutation, and 4 elites. Each chromosome is encoded with the order of machining regions, contour direction, entry point code, linking sequence code, and corner transition. The initial generation is created using random feasible NX reference path configurations.

DOI: 10.54254/2755-2721/2026.34321

The fitness function includes the objective function and penalties. The penalty scheme consists of five terms based on region coverage, non-collision, corner angle limit, path continuity, and machine movement limit. Generation 120 stops the simulation or the optimal objective function stops changing by more than 0.001 for 15 successive generations.

4. Experimental procedure

4.1. Machine setup and path generation workflow

VMC 850 machining center has a 6 mm polycrystalline diamond end mill. The same fixture origin and tool-length compensation are applied across all trials. For each model, Siemens NX generates one reference path. The path file is exported to MATLAB and converted into point-segment format. Node selection is performed at 2 mm spacing. Cutting, linking, entry, and exit segments are labeled. The energy model and carbon-emission calculation rule are imported into MATLAB. The genetic algorithm generates an optimized low-carbon path for each model. The optimized path is then rechecked against coverage, collision, angle, continuity, and machine-limit constraints before machining.

4.2. Data processing and carbon evaluation

The WT5000 records instantaneous power at 0.1 s intervals during the complete machining cycle. CNC axis-motion logs are exported after each trial and synchronized with power data using Python 3.11. Timestamp correction is performed by matching spindle-start and spindle-stop markers. Power curves are segmented into cutting, rapid traverse, linking, and idle phases according to CNC log states. Cutting energy, rapid-traverse energy, and idle energy are calculated separately from the segmented power curves. Total energy is obtained by summing all phase-level energy values. Carbon emission is calculated by multiplying electrical energy by the fixed emission factor of 0.570 kg CO_2/kWh. MATLAB calculates path features, including total path length, non-cutting length, number of sharp turns, maximum corner angle, average transition angle, and local curvature variation. Edge-defect length is extracted from Keyence VHX-7000 images through grayscale thresholding and contour measurement. Each reference-path trial and optimized-path trial is stored in a paired comparison table.

4.3. Comparative experiment and output configuration

The experiment has two fixed groups: NX reference path and optimized low-carbon path. Every one of the 30 work pieces is machined three times on the reference path and once with the optimized path, resulting into 60 full trials. Both groups use the same tool, machine, spindle speed, feed rate, depth of cut, coordinate system, inspection procedure, and power-measurement setup. The output indicators include machining time, energy usage, carbon footprint, non-cutting distance, mean spindle power, surface roughness Ra and length of edge defect. The statistical comparison is performed in python through pandas, numpy, scipy and matplotlib.

DOI: 10.54254/2755-2721/2026.34321

5. Experimental results

5.1. Geometric characteristics of aerospace composite parts and path statistics

The 30 CFRP bracket design models were quite geometrically variable. In particular, the mean length of the outer contour was found to be 684.3 plus or minus 76.5 mm, the length of the slot contour was found to be 214.7 ± 31.2 mm, and the complexity index of the boundary was found to be 0.463 plus or minus 0.082 (see Figure 2). The optimized trajectory decreased the overall path length by an average of 1286.5 ± 108.4mm to 1000.1 ± 92.6mm** as compared to the NX reference trajectory, and also minimized the non-cutting path length of 426.3 ± 57.8mm to 211.5 ± 43.1mm***.

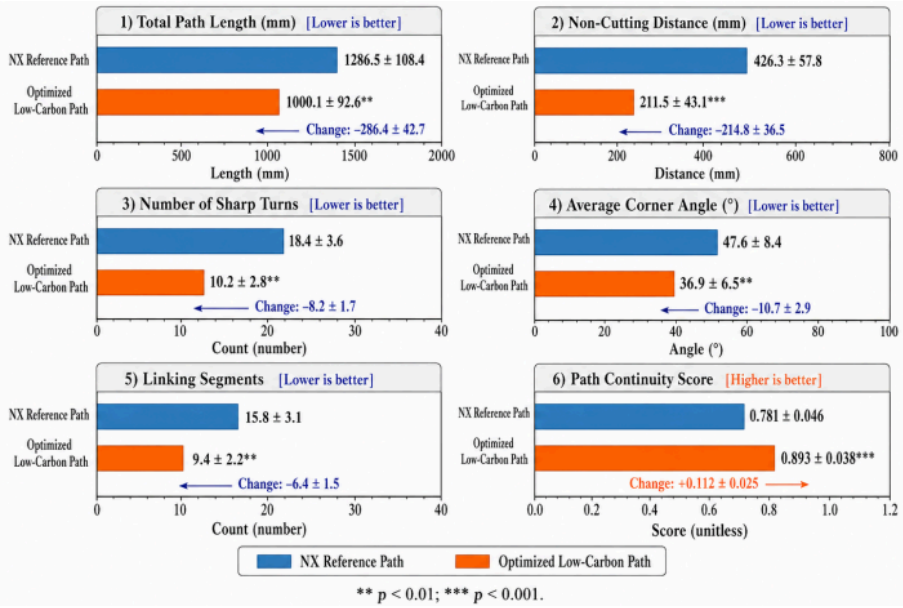

Figure 2. Geometric characteristics and path statistics

5.2. Comparative results of machining time, energy consumption, and carbon emission

The optimal path reduced the processing time from 142.8 ± 12.6 seconds to 124.2 ± 10.9 seconds**, while the total energy expenditure dropped from 0.912 ± 0.086 kWh to 0.728 ± 0.071 kWh***. Emissions of carbon dioxide gas were lowered from 0.520 ± 0.049 kilograms to 0.415 ± 0.041 kilograms***. The average spindle power underwent a relatively small reduction, from 1.86 ± 0.18 kilowatts to 1.79 ± 0.16 kilowatts*, meaning that energy was mainly conserved by minimizing idle time and reducing processing time.

5.3. Surface quality, edge integrity, and overall path-planning performance

The optimized path maintained machining quality while reducing carbon indicators. Surface roughness Ra changed from 1.46 ± 0.17 μm to 1.42 ± 0.16 μm, and edge-defect length decreased from 3.84 ± 0.72 mm to 3.21 ± 0.61 mm*. The overall low-carbon performance index increased by +0.164 ± 0.032*** (see Table 1). The mechanism is that reducing linking distance and sharp transitions lowers idle and rapid-traverse energy, while smoother corner strategy limits local edge damage. Carbon reduction is therefore produced by path-structure optimization rather than by weakening machining quality.

DOI: 10.54254/2755-2721/2026.34321

Table 1. Energy, carbon, and surface-quality comparison

Indicator	NX Reference Path	Optimized Low-Carbon Path	Change
Machining Time (s)	142.8 ± 12.6	124.2 ± 10.9**	−18.6 ± 3.9
Total Energy Consumption (kWh)	0.912 ± 0.086	0.728 ± 0.071***	−0.184 ± 0.037
Carbon Emission (kg CO_2)	0.520 ± 0.049	0.415 ± 0.041***	−0.105 ± 0.021
Average Spindle Power (kW)	1.86 ± 0.18	1.79 ± 0.16*	−0.07 ± 0.03
Surface Roughness Ra (μm)	1.46 ± 0.17	1.42 ± 0.16	−0.04 ± 0.02
Edge-Defect Length (mm)	3.84 ± 0.72	3.21 ± 0.61*	−0.63 ± 0.24
Low-Carbon Performance Index	0.684 ± 0.051	0.848 ± 0.043***	+0.164 ± 0.032

6. Conclusion

This study establishes a low-carbon intelligent machining path planning framework for lightweight CFRP aerospace components. The framework integrates Siemens NX geometric modeling, path segmentation, energy-consumption modeling, carbon-emission calculation, genetic-algorithm optimization, machine-side power measurement, and post-machining quality inspection. The optimized path reduces total path length, non-cutting distance, sharp turns, machining time, energy consumption, and carbon emission under fixed machining parameters. The results show that low-carbon improvement is achieved mainly through path-structure adjustment. Shorter linking paths reduce idle and rapid-traverse energy, smoother corner transitions reduce unnecessary motion fluctuation, and complete region coverage maintains machining quality. Surface roughness remains stable, while edge-defect length slightly decreases.

References

[1] Shokrani, A., Arrazola, P. J., Biermann, D., Mativenga, P., & Jawahir, I. S. (2024). Sustainable machining: Recent technological advances. CIRP Annals, 73(2), 483–508.
[2] Slamani, M., & Chatelain, J.-F. (2023). A review on the machining of polymer composites reinforced with carbon (CFRP), glass (GFRP), and natural fibers (NFRP). Discover Mechanical Engineering, 2, Article 4.
[3] Jiao, J., Cheng, X., Wang, J., Sheng, L., Zhang, Y., Xu, J., Jing, C., Sun, S., Xia, H., & Ru, H. (2023). A review of research progress on machining carbon fiber-reinforced composites with lasers. Micromachines, 14(1), 24.
[4] Tima, T. S., Geier, N., & Szalay, T. (2024). Machining-induced burr suppression in edge trimming of carbon fibre-reinforced polymer (CFRP) composites by tool tilting. Journal of Manufacturing and Materials Processing, 8(6), 247.
[5] Pajaziti, A., Tafilaj, O., Gjelaj, A., & Berisha, B. (2025). Optimization of toolpath planning and CNC machine performance in time-efficient machining. Machines, 13(1), 65.
[6] Wu, L., Zhang, Y., Zhang, M., Cui, X., Zhang, F., Gong, P., Liu, M., Yang, M., Dambatta, Y. S., & Li, C. (2025). Carbon emission in manufacturing processes: Modeling and evaluation. Frontiers of Mechanical Engineering, 20, Article 28.
[7] Qu, W., Chen, Y., Xu, J., & Huang, Z. (2025). Low-carbon, high-efficiency, and high-quality equipment selection for milling process based on new quality productivity orientation. Processes, 13(9), 2935.
[8] Xiang, Q., Ding, W., & Xing, S. (2025). Energy-saving and low-emission equipment selection for machining process based on new quality productivity orientation. Processes, 13(11), 3437.
[9] Jiang, P., Wang, Z., Li, X., Wang, X. V., Yang, B., & Zheng, J. (2023). Energy consumption prediction and optimization of industrial robots based on LSTM. Journal of Manufacturing Systems, 70, 137–148.
[10] Muru, J., & Rassõlkin, A. (2025). A scoping review of energy consumption in industrial robotics. Machines, 13(7), 542.